Coherent backscattering by airless Solar System objects using Mueller matrix decomposition

Karri Muinonen[1,2]
Professor of Astronomy
[1]Department of Physics, University of Helsinki, Finland
[2]Finnish Geospatial Research Institute (FGI), Masala, Finland

Acknowledgments: Academy of Finland
European Research Council,

Astrophysics Seminar, Department of Physics, University of Helsinki, May 7, 2021

Contents

- Introduction
- Multiple scattering
  - Numerical methods
  - Radiative transfer and coherent backscattering (RT-CB)
  - Radiative transfer with reciprocal transactions (R^2T^2)
  - Validation of numerical methods
- Mueller matrix decomposition
- Granada-Amsterdam Light Scattering Database
  - Cosmic Dust Laboratory (CoDuLab) experimental measurements
  - Basalt scattering matrix
- Lunar scattering model
  - Lunar phase curve: first results
  - Lunar polarization ratios: first results
- Conclusions with future prospects

Introduction

- Physical characterization of the surfaces of airless planetary objects
- Direct problem of light scattering by discrete random media of particles with varying particle size, shape, refractive index, and volume density
- Inverse problem based on astronomical observations and/or experimental measurements
- Plane of scattering, scattering angle, solar phase angle, degree of linear polarization

By Gregory H. Revera

Polarimetric & photometric observations

Moon

Photometry

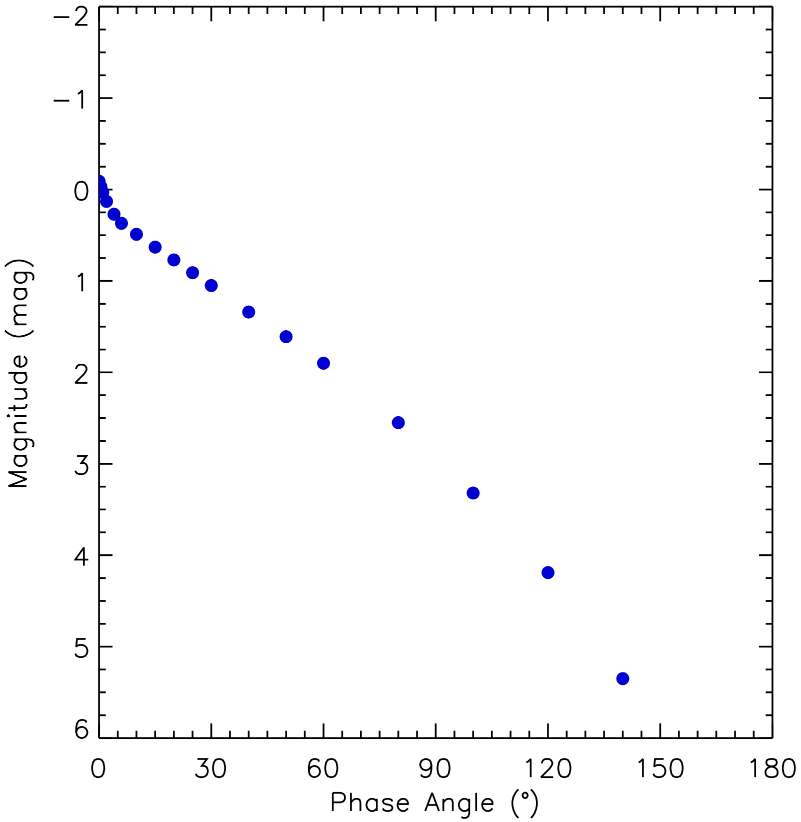

Polarimetry

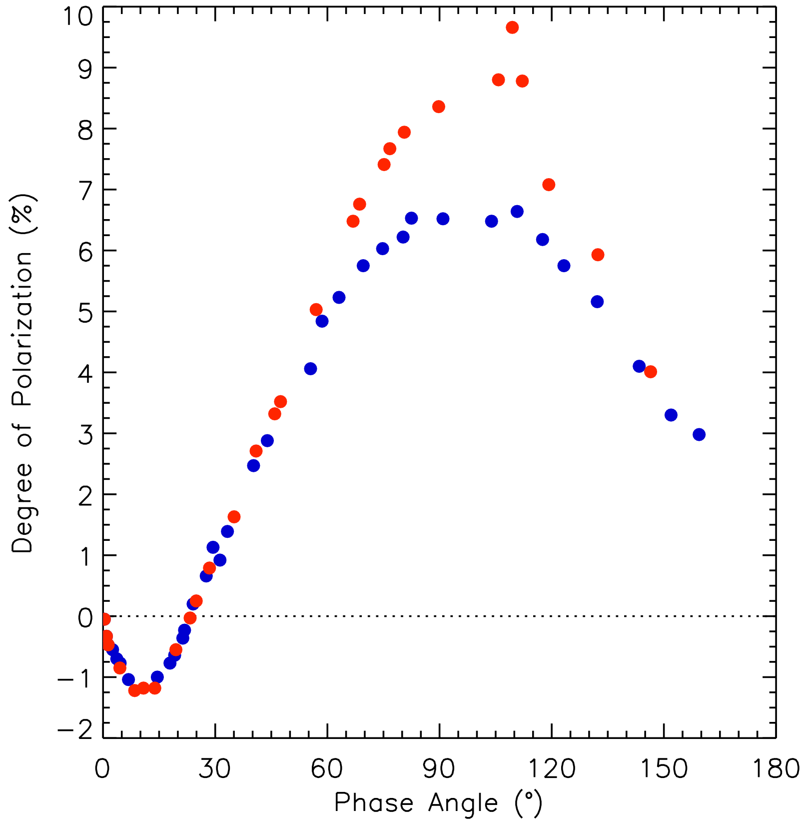

Rougier (1933), Lyot (1929)

Asteroids

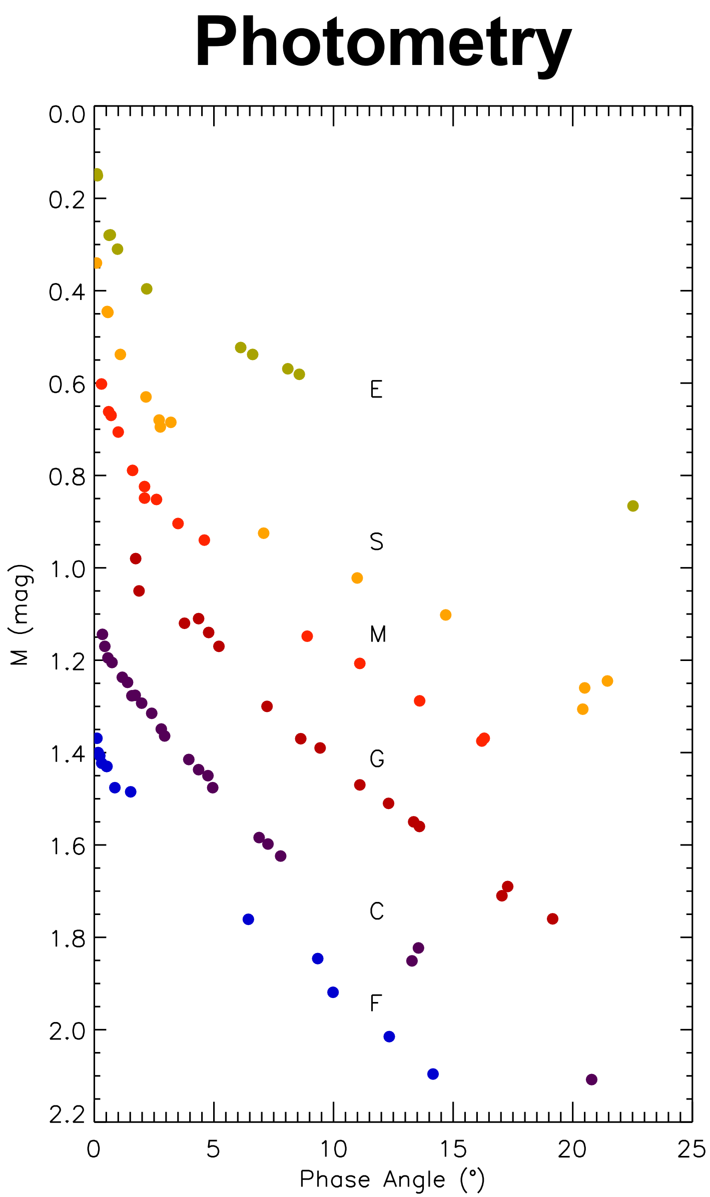

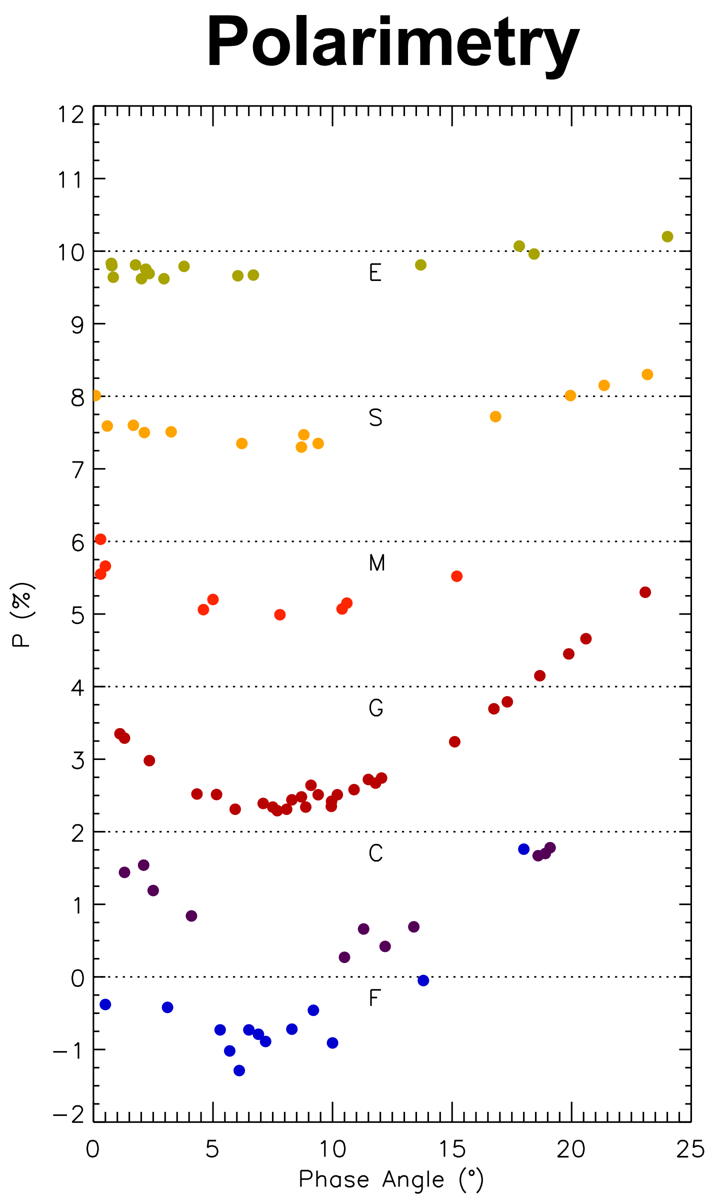

Muinonen et al., in Polarimetry of Stars and Planetary Systems, 2016 (obs. ref. therein)

Coherent backscattering mechanism: intensity

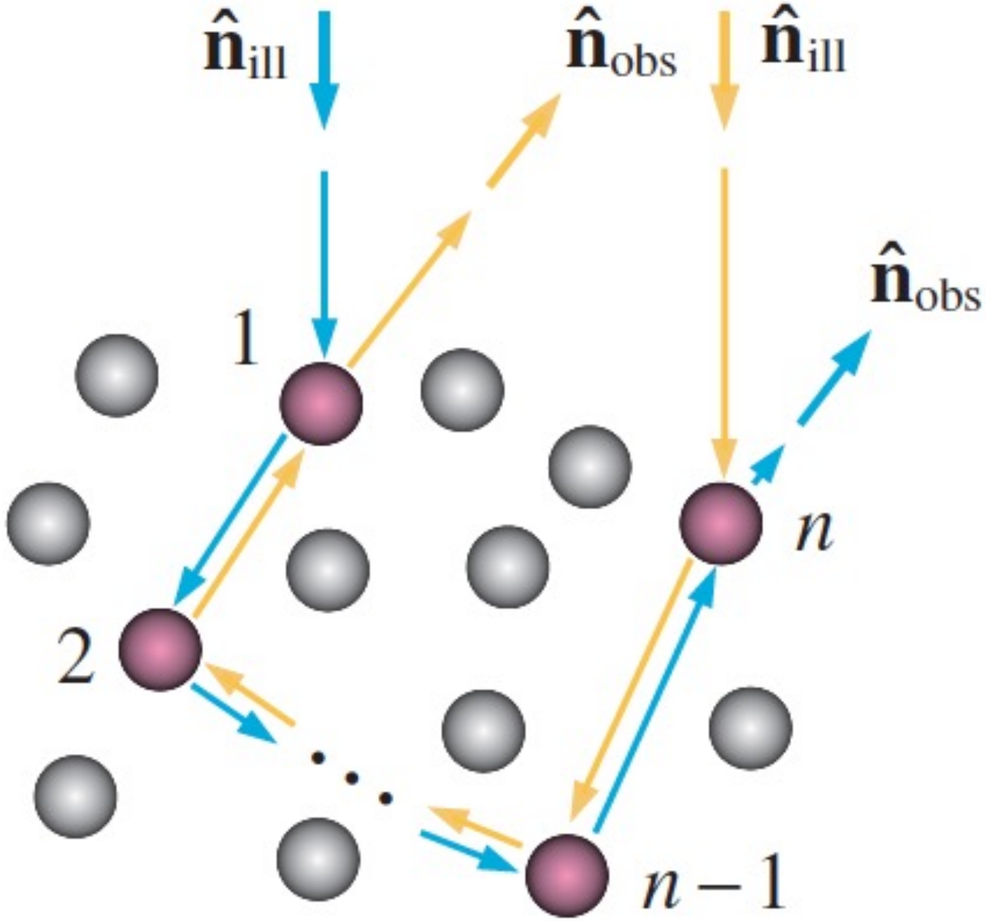

e.g., Muinonen 1989, 1990; Shkuratov 1985, 1988, 1989

Coherent backscattering mechanism: polarization

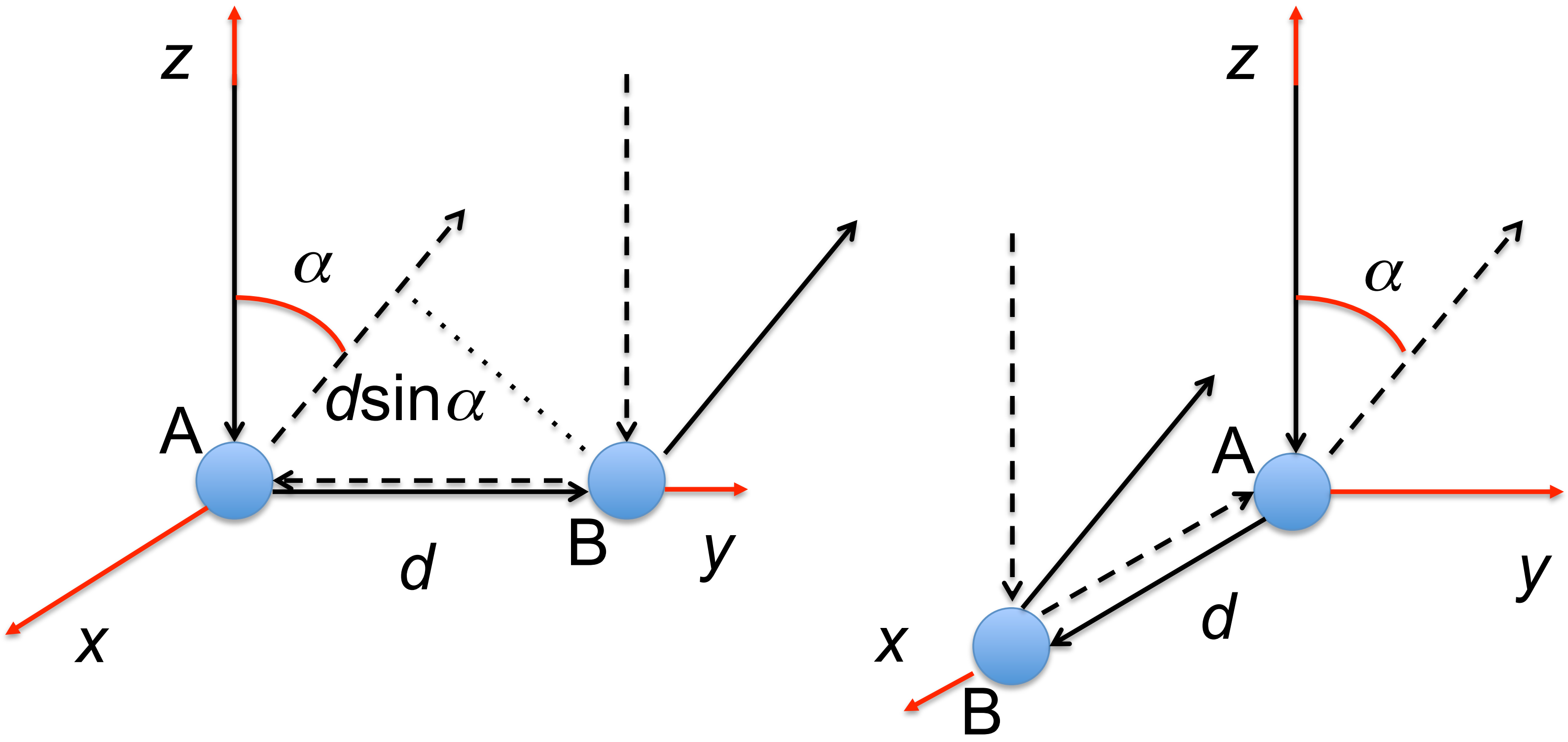

Muinonen 1989, 1990; Shkuratov 1985, 1988, 1989

Multiple scattering

- Radiative transfer and coherent backscattering (RT-CB; Muinonen et al., ApJ 2012; Muinonen, WRM 2004 and URSI EMTS 1989)
- Superposition *T*-Matrix Method (STMM or MSTM; Mackowski & Mishchenko, JQSRT 2011; FaSTMM, Markkanen & Yuffa JQSRT 2017)
- Electric Current Volume Integral Equation Method (JVIE; Markkanen & Yuffa, JQSRT 2017, Markkanen et al., IEEE-TAP 2012)
- Radiative transfer with reciprocal transactions (R^2T^2; Muinonen et al., URSI EMTS 2016ab, RS 2017, OL 2018, JoVE 2019; Markkanen et al., OL 2018, ApJL 2018; Väisänen et al., PLoS ONE 2019)

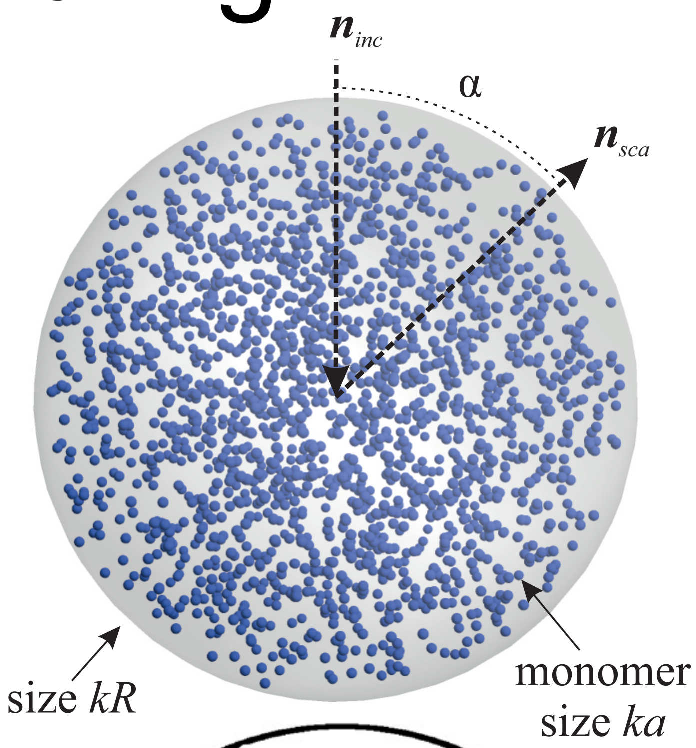

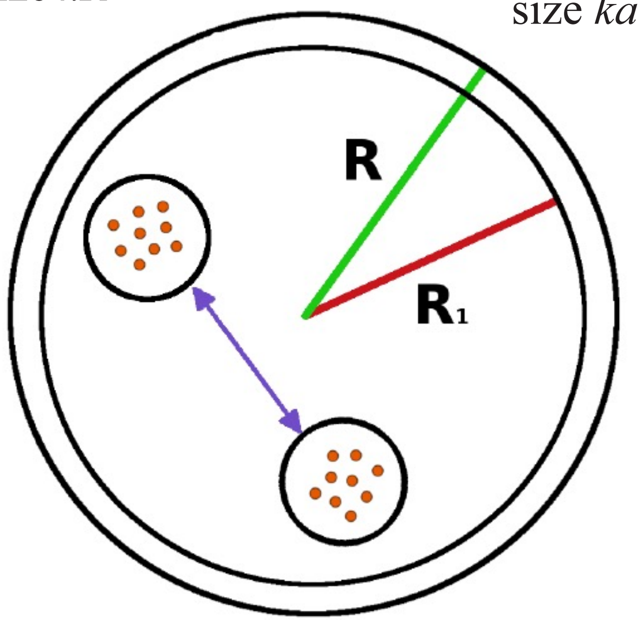

$$\boldsymbol{I}_{\mathrm{i}} = (I_{\mathrm{i}}, Q_{\mathrm{i}}, U_{\mathrm{i}}, V_{\mathrm{i}})^T$$

$$\boldsymbol{I}_{\mathrm{s}} = (I_{\mathrm{s}}, Q_{\mathrm{s}}, U_{\mathrm{s}}, V_{\mathrm{s}})^T$$

$$\boldsymbol{I}_{\mathrm{s}} = \frac{1}{k^2 R^2}\, \boldsymbol{S} \cdot \boldsymbol{I}_{\mathrm{i}}$$

(Here R is the distance between observer and scatterer.)

$$\mu_{\mathrm{L}} = \frac{P_{11} - P_{22}}{P_{11} + 2P_{21} + P_{22}}.$$

$$\mu_{\mathrm{C}} = \frac{P_{11} + P_{44}}{P_{11} - P_{44}}.$$

Muinonen et al. 2012

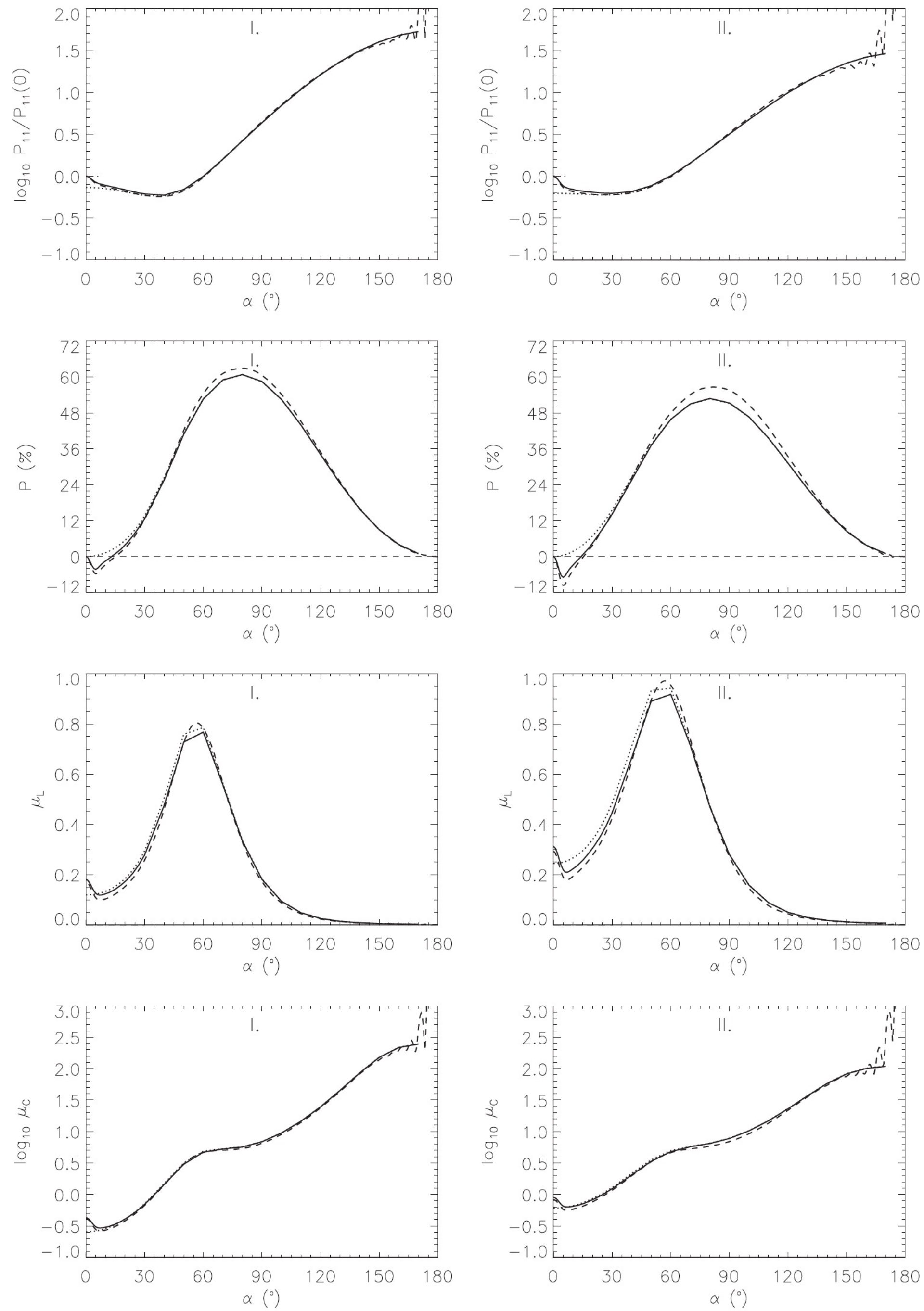

Figure 3. Same as in Figure 2, but for the full range of phase angles.

Comparison with JVIE

- R^2T^2, exact incoherent interactions using *T*-matrices from JVIE (Markkanen et al., Optics Letters 2018)
- Spherical media, radius $kR = 60$, Voronoi media:
  - Case I, Ice:
    - radius $kr = 2.0$, refractive index $m = 1.31$
    - volume densities $v = 0.125, 0.25$
- Spherical media, radius $kR = 1.2 \times 10^{13}$ (!):
  - Case II, Silicate:
    - radius $kr = 1.5$, refractive index $m = 1.8 + i0.000188$
    - volume densities $v = 0.15, 0.30$

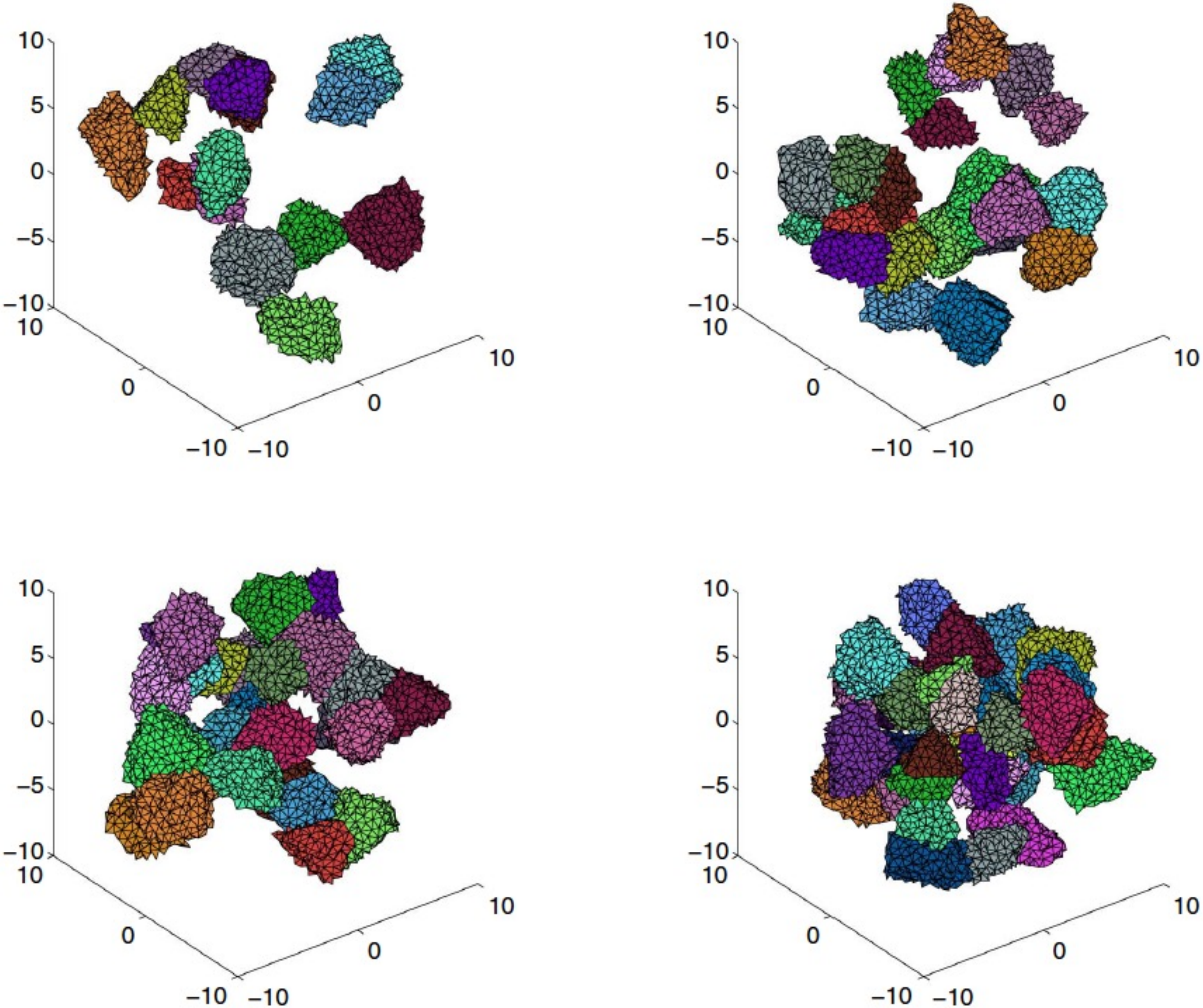

10
5
0
−5
−10
10
0
−10
−10
0
10
10
5
0
−5
−10
10
0
−10
−10
0
10
10
5
0
−5
−10
10
0
−10
−10
0
10
10
5
0
−5
−10
10
0
−10
−10
0
10

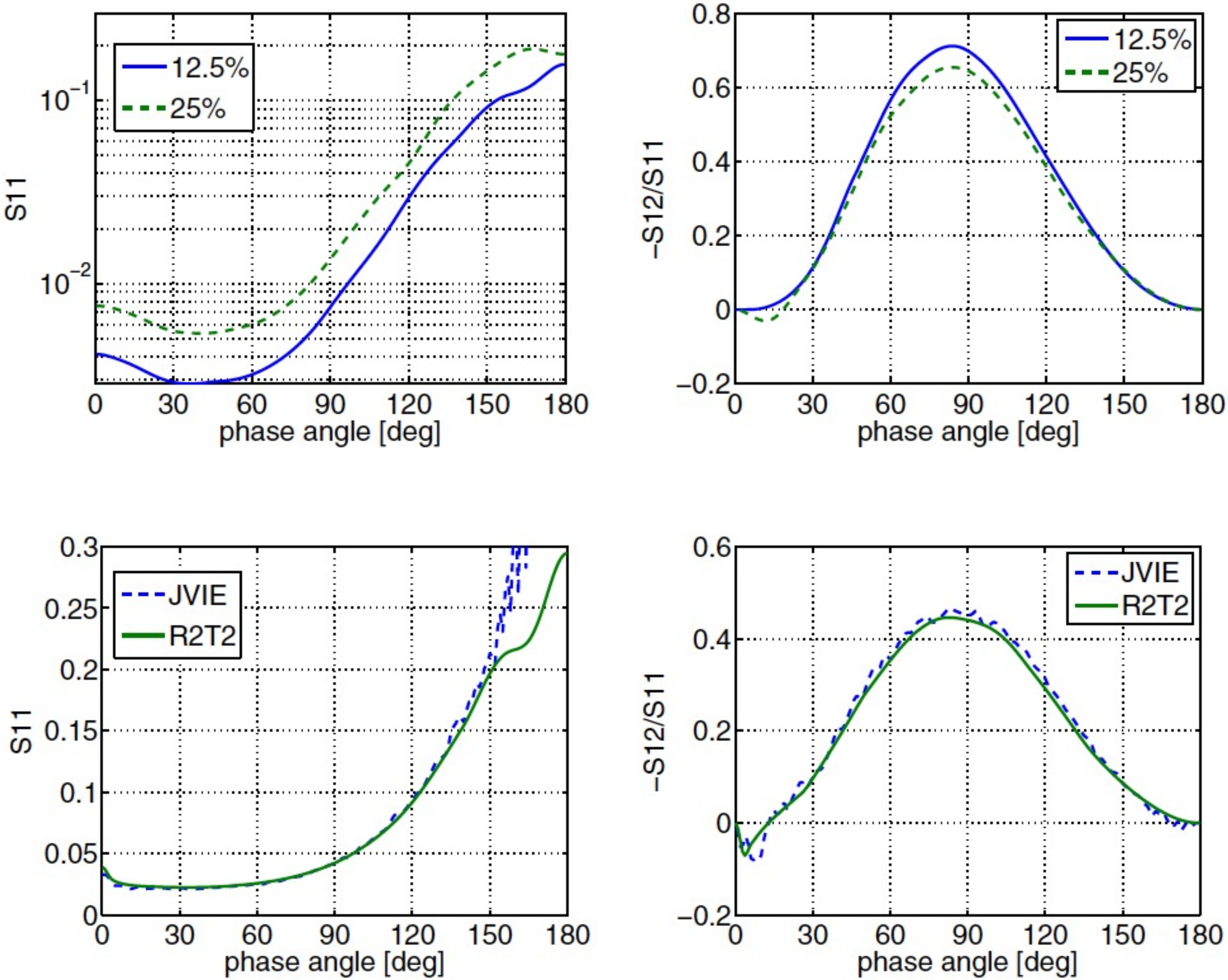
12.5%
25%
S11
phase angle [deg]
−S12/S11
JVIE
R2T2

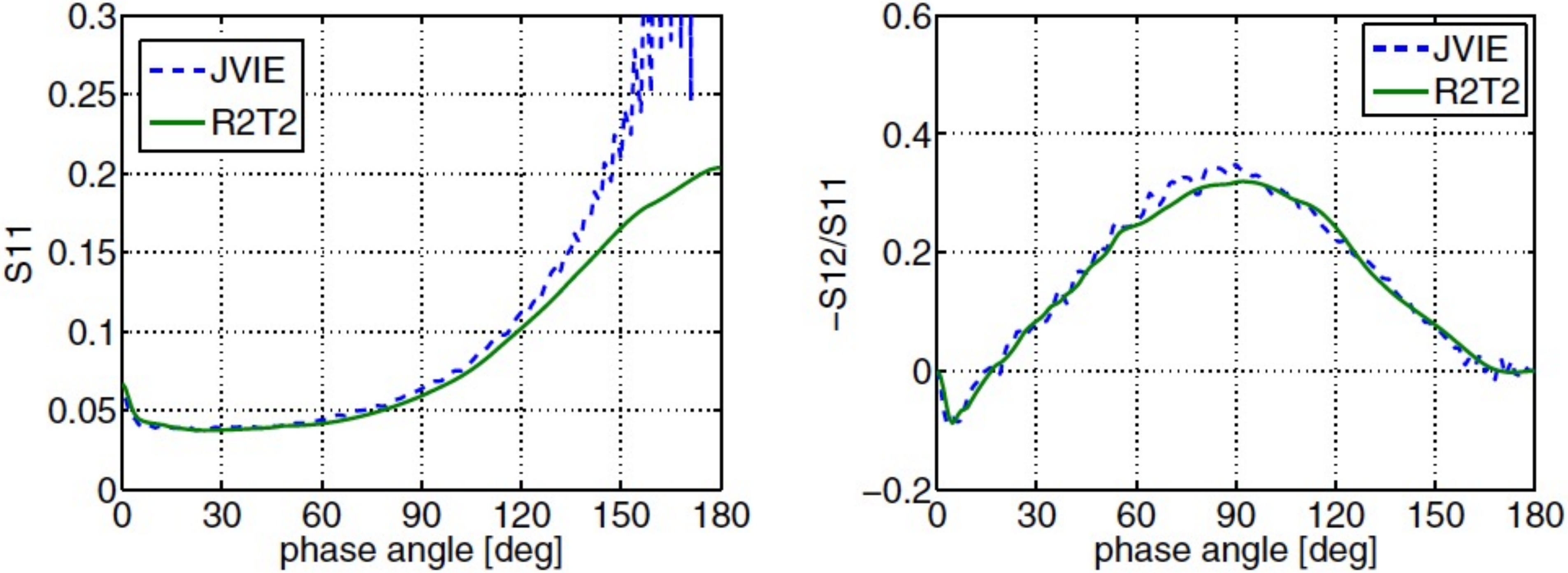

0.3
0.25
0.2
0.15
0.1
0.05
0
S11
JVIE
R2T2
0
30
60
90
120
150
180
phase angle [deg]
0.6
0.4
0.2
0
−0.2
−S12/S11
JVIE
R2T2
0
30
60
90
120
150
180
phase angle [deg]

Mueller matrix decomposition

- RT-CB requires amplitude scattering matrices
- amplitude scattering matrices give rise to pure Mueller matrices
- from pure Mueller matrices, amplitude matrices derived for each scattering angle without absolute electromagnetic phase
- Cloude (1986, 1990) superpositional decomposition into four pure 4 x 4 Mueller matrices
- Presently, superpositional decomposition into six pure Mueller matrices

Granada-Amsterdam Light Scattering Database
CoDuLab experimental measurements

- Basalt sample
  - Tenerife, volcanic eruption
- pyroxene (augite), plagioclase, olivine
- particle effective sizes 3-7 μm
- Particle refractive index
  - 1.52 + i0.00092 at 488 nm
  - 1.52 + i0.001 at 647 nm
- Appearance as powder
  - dark grey
- References
  - Muñoz et al. 2012
  - Dabrowska et al. 2015
  - Pollack et al. 1973

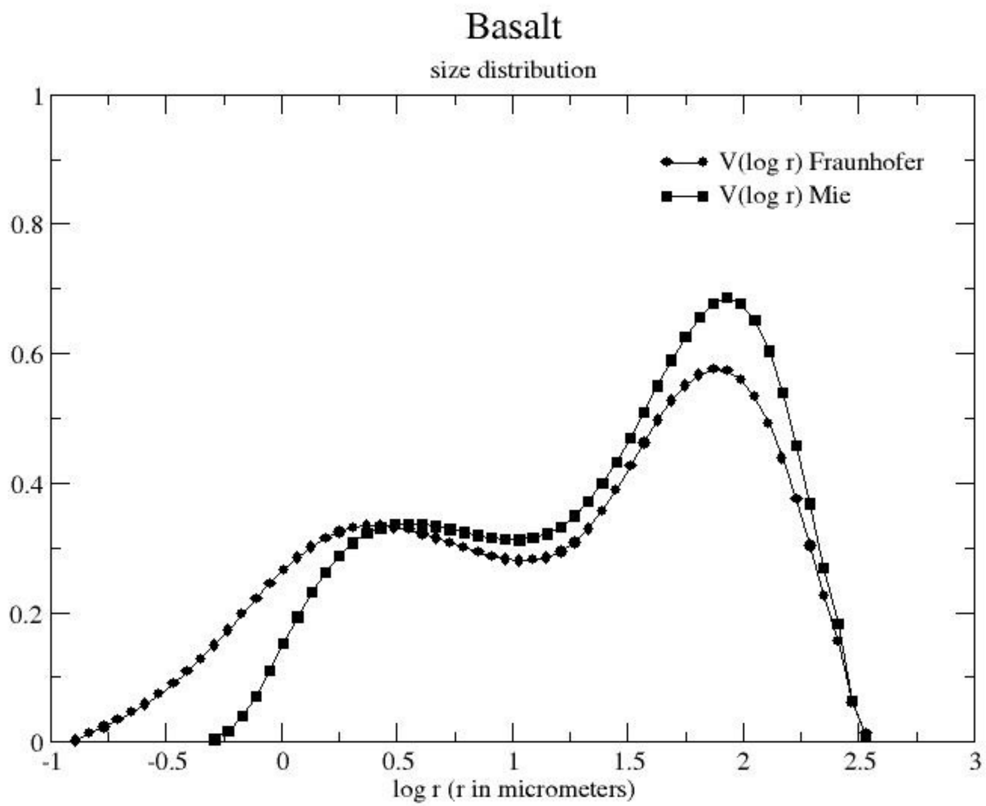

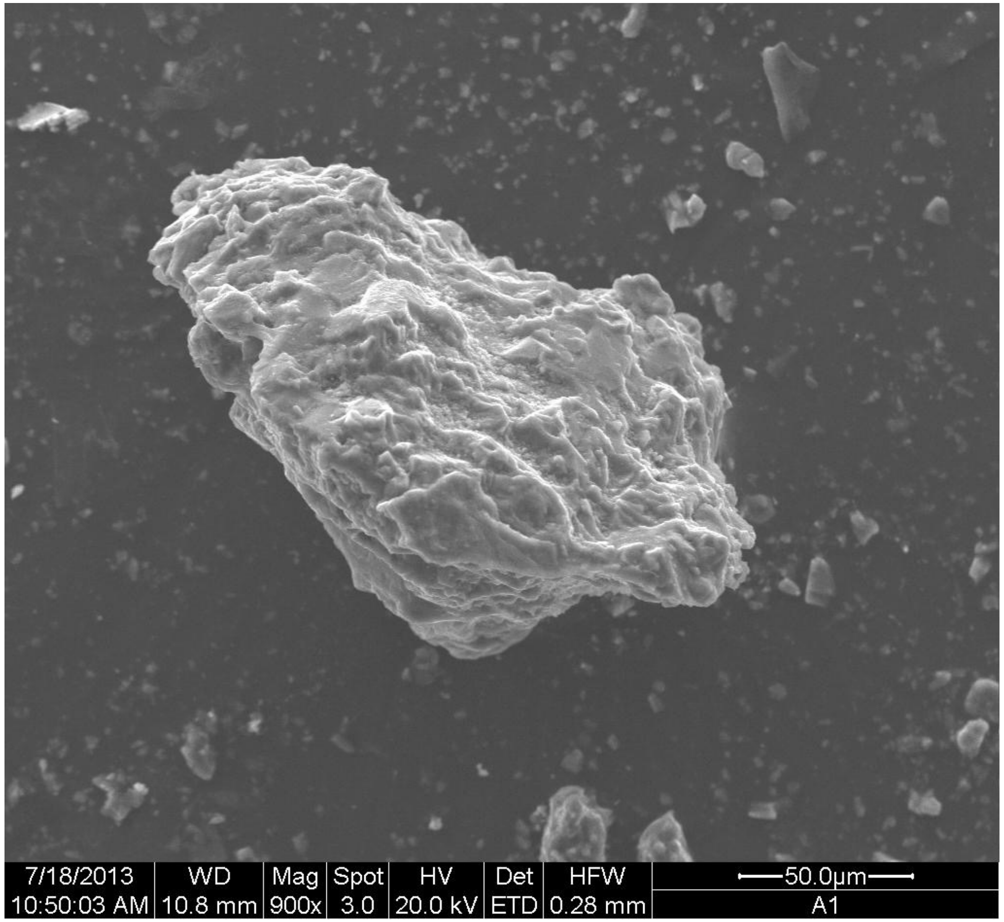
7/18/2013
10:50:03 AM
WD
10.8 mm
Mag
900x
Spot
3.0
HV
20.0 kV
Det
ETD
HFW
0.28 mm
50.0µm
A1

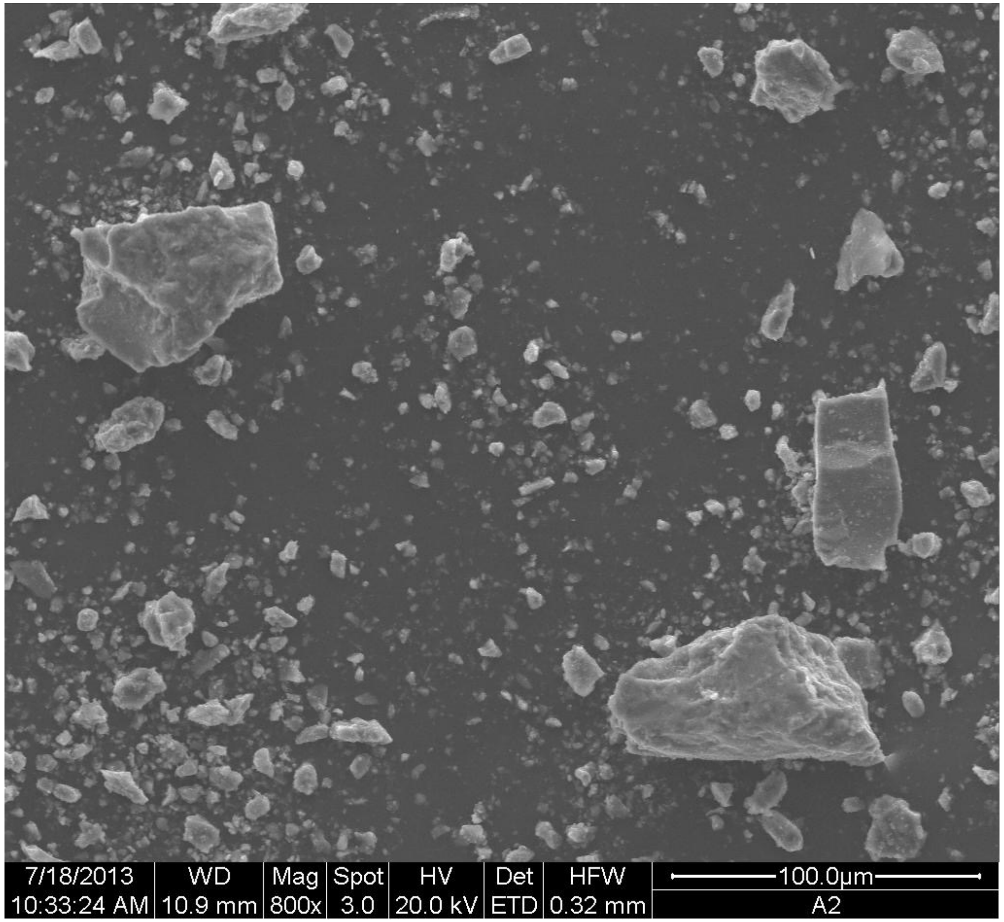
7/18/2013
10:33:24 AM
WD
10.9 mm
Mag
800x
Spot
3.0
HV
20.0 kV
Det
ETD
HFW
0.32 mm
100.0µm
A2

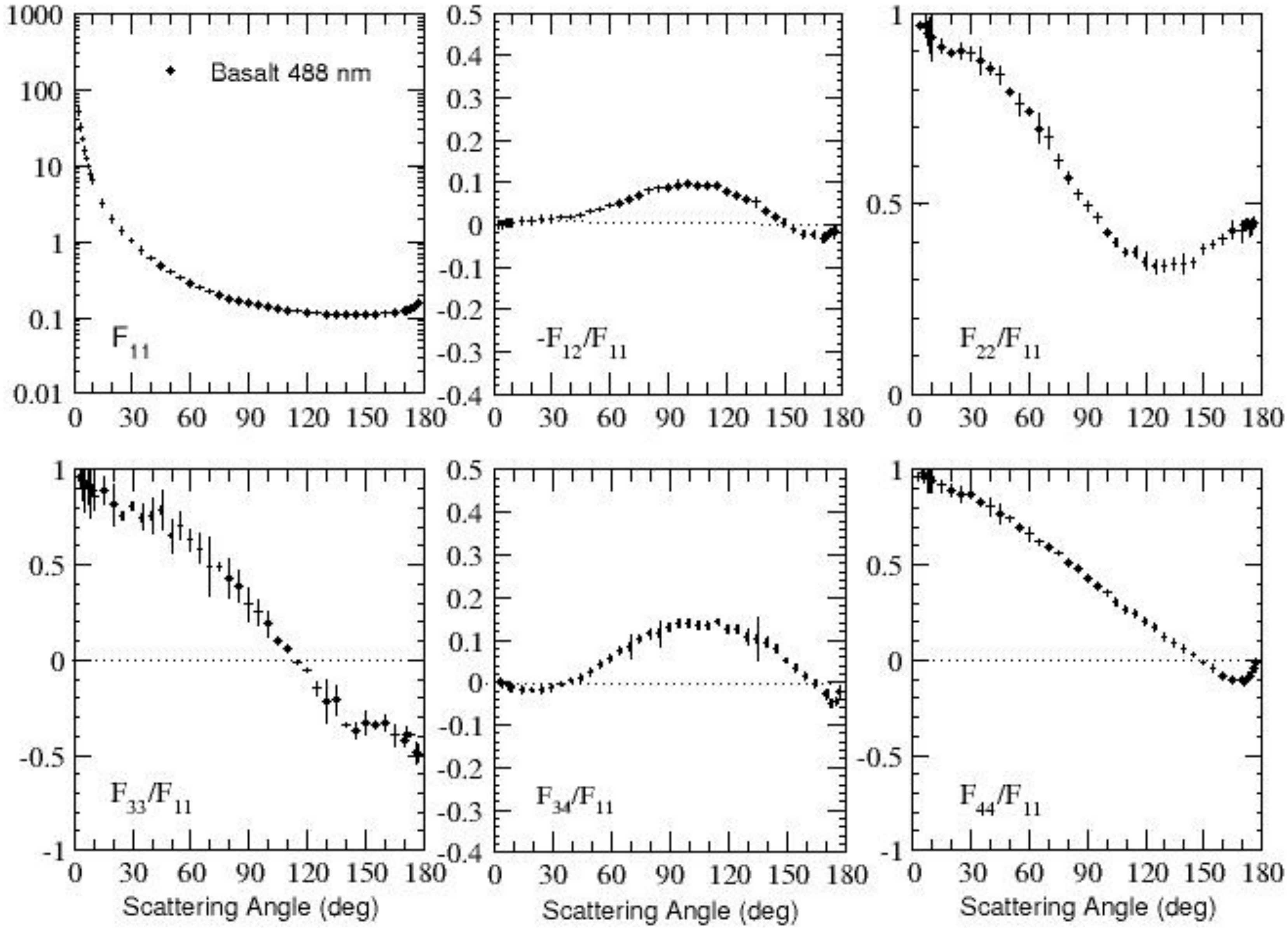
Basalt 488 nm
F11
-F12/F11
F22/F11
F33/F11
F34/F11
F44/F11
Scattering Angle (deg)
Scattering Angle (deg)
Scattering Angle (deg)

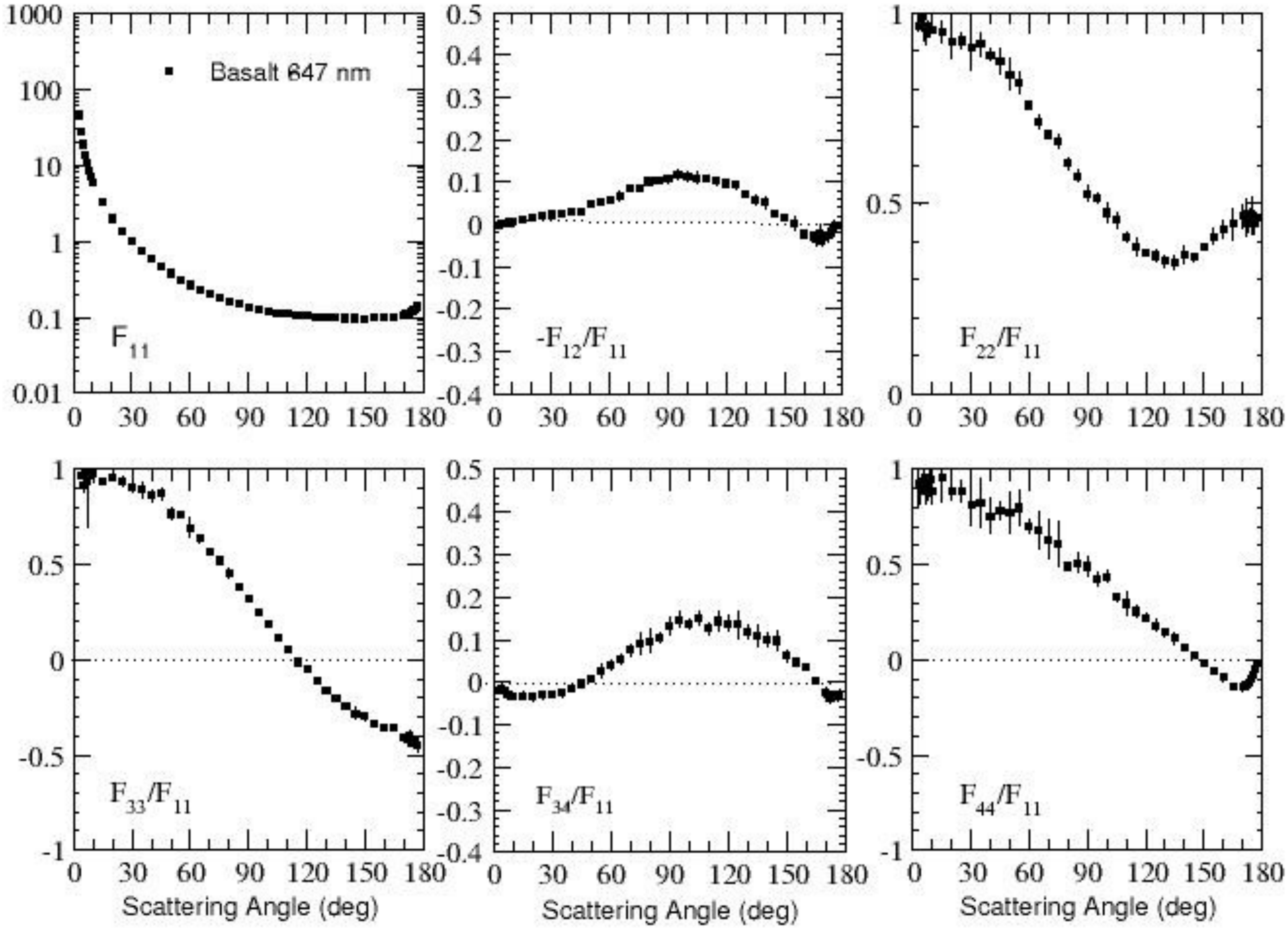
Basalt 647 nm
F_{11}
$-F_{12}/F_{11}$
F_{22}/F_{11}
F_{33}/F_{11}
F_{34}/F_{11}
F_{44}/F_{11}
Scattering Angle (deg)
Scattering Angle (deg)
Scattering Angle (deg)

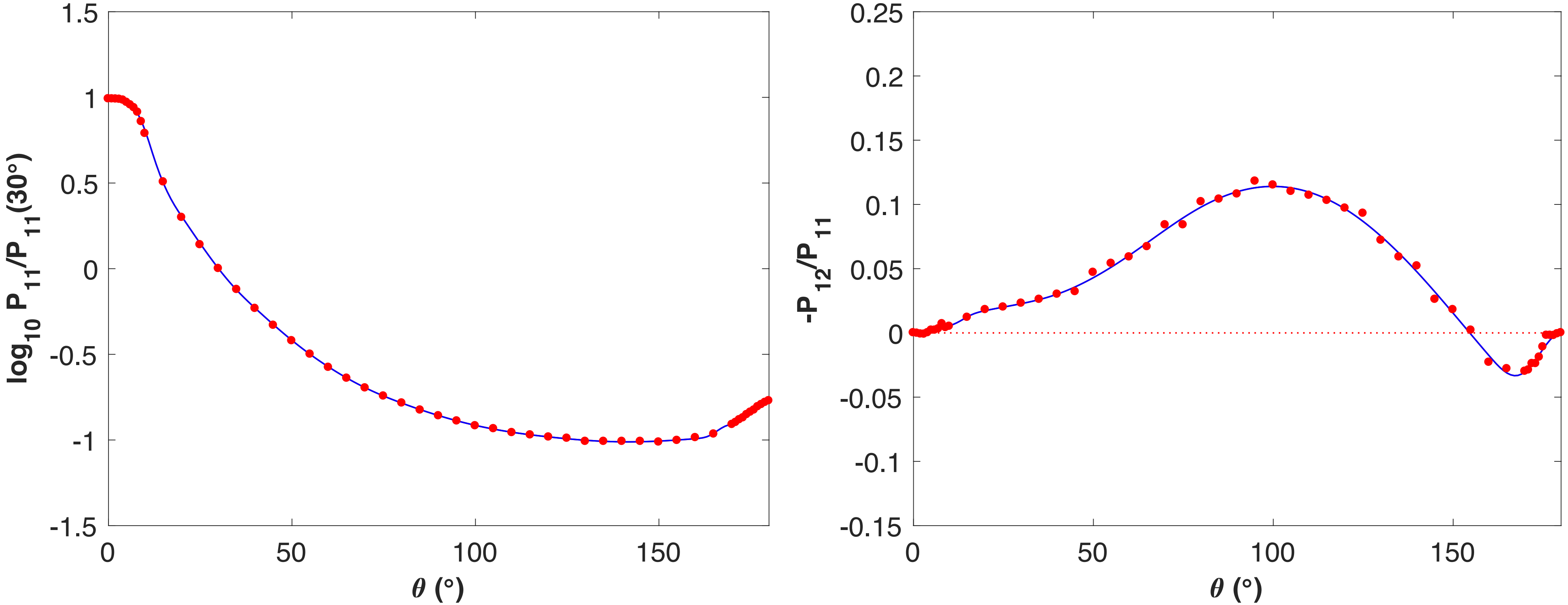

1.5
1
0.5
0
-0.5
-1
-1.5
log10 P11/P11(30°)
0
50
100
150
θ (°)
0.25
0.2
0.15
0.1
0.05
0
-0.05
-0.1
-0.15
-P12/P11
0
50
100
150
θ (°)

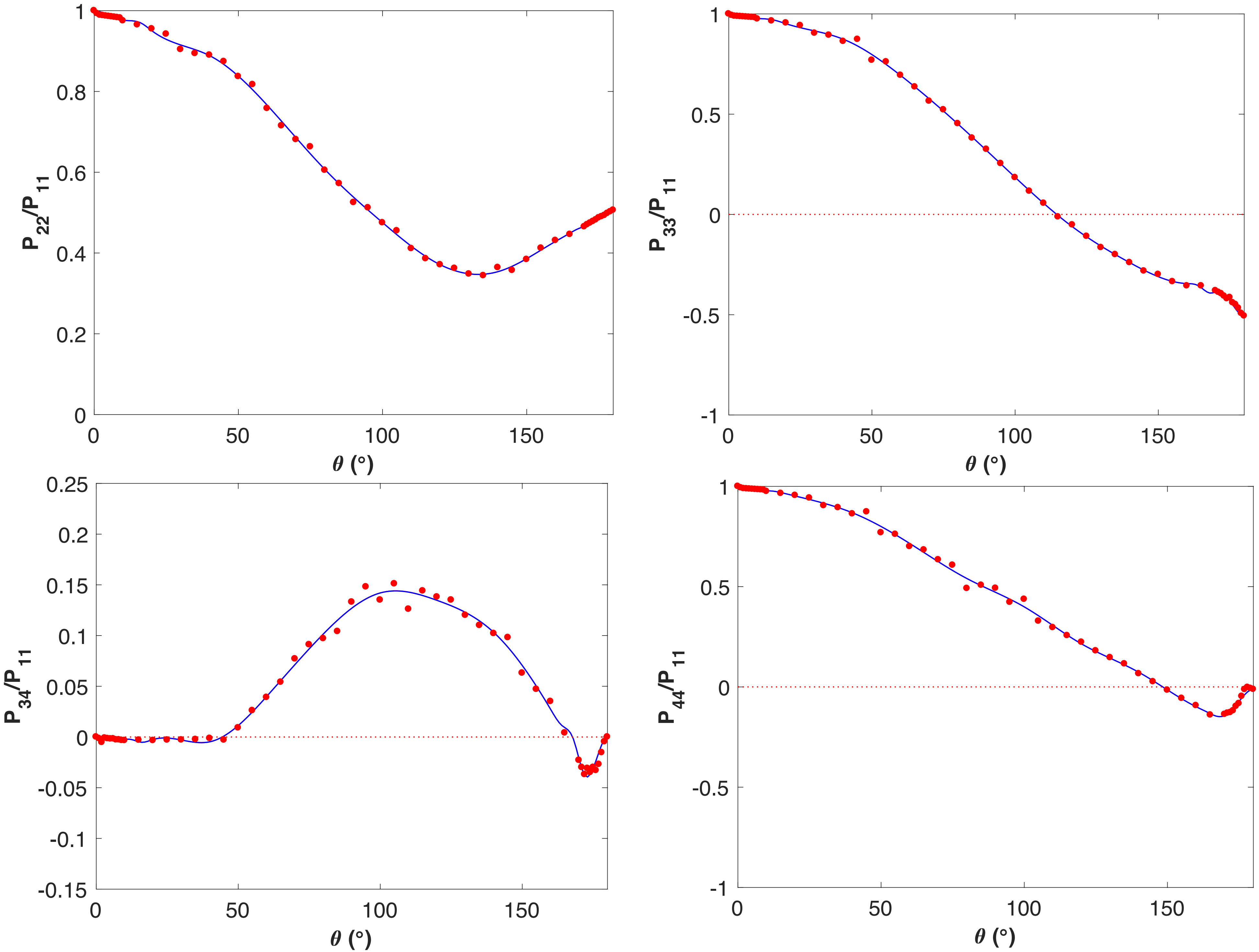

P22/P11
P33/P11
P34/P11
P44/P11
θ (°)
θ (°)
θ (°)
θ (°)

Zubko et al. 2013, feldspar, 632 nm

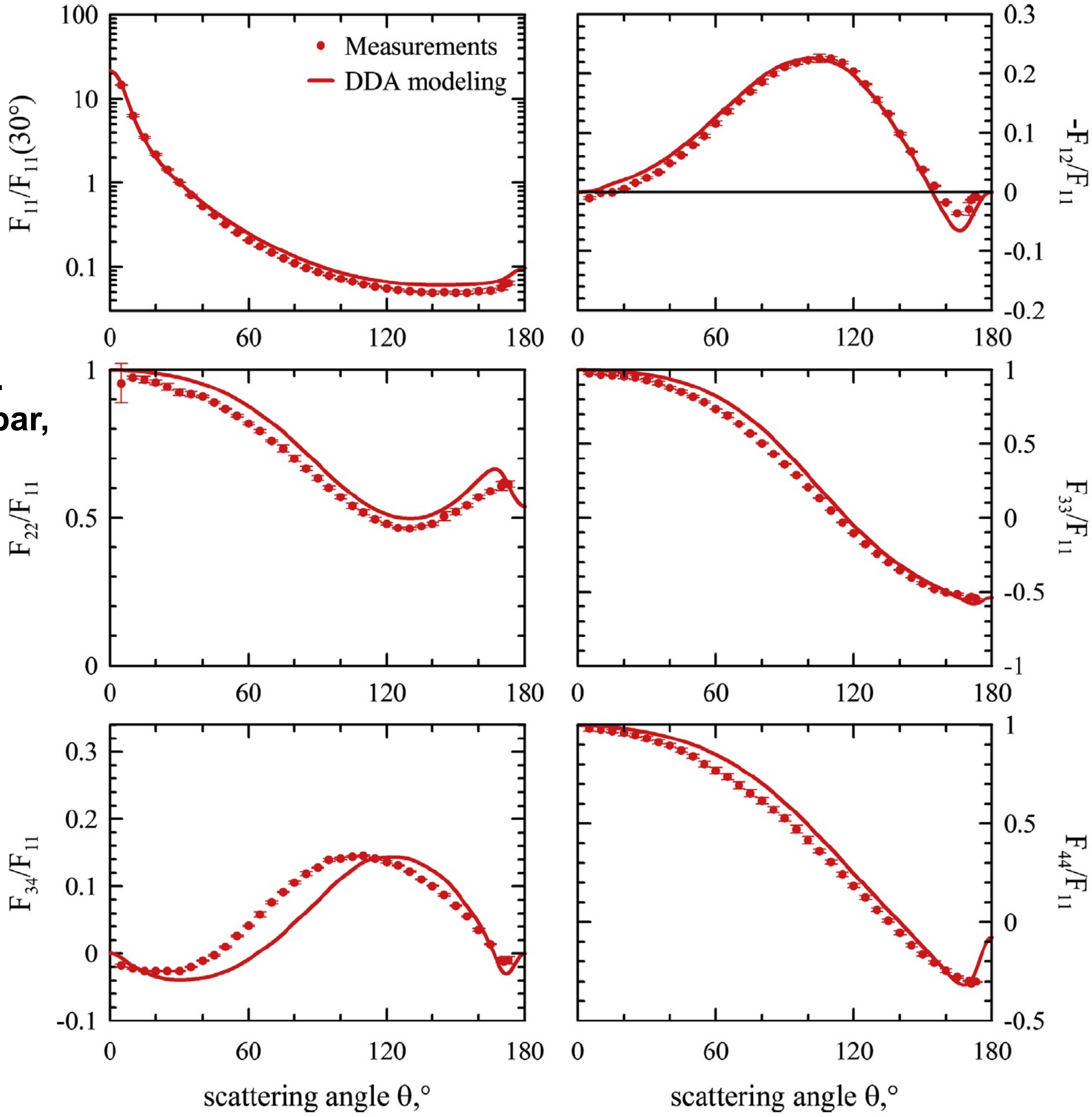

Lunar scattering model

RT-CB computations with modified basalt input

- “Infinite” spherical medium of modified basalt scatterers
- Incoherent input, forward diffraction excluded
- Modified scattering phase matrix accurately decomposed into pure Mueller matrices
- Lunar geometric albedo 0.136 obtained with input single-scattering albedo of 0.723
- Lunar opposition effect angular width matched with mean free path of 4 μm
- $-P_{12}/P_{11}$ in single scattering iterated for best fit with the lunar polarization

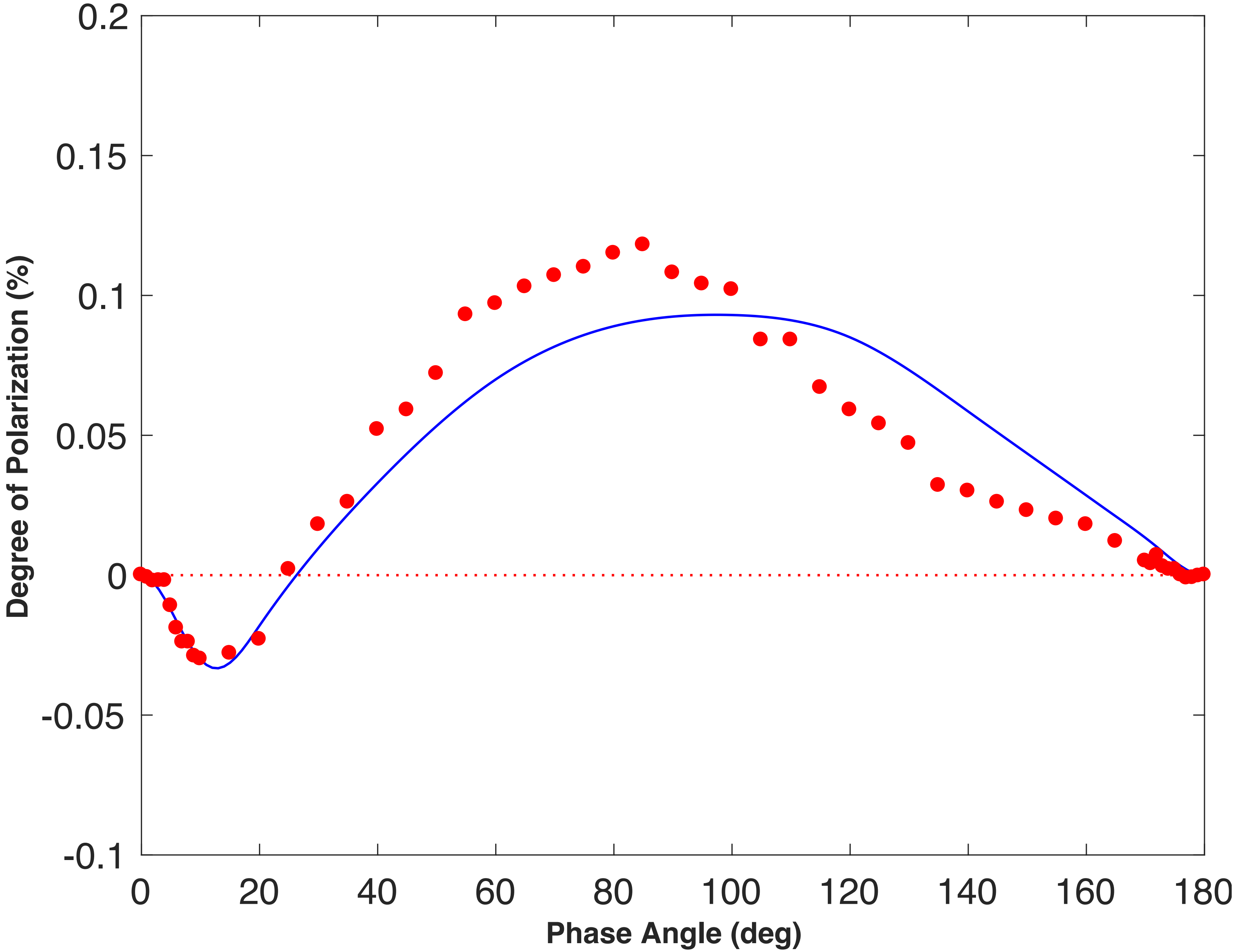

0.2
0.15
0.1
0.05
0
-0.05
-0.1
0
20
40
60
80
100
120
140
160
180
Degree of Polarization (%)
Phase Angle (deg)

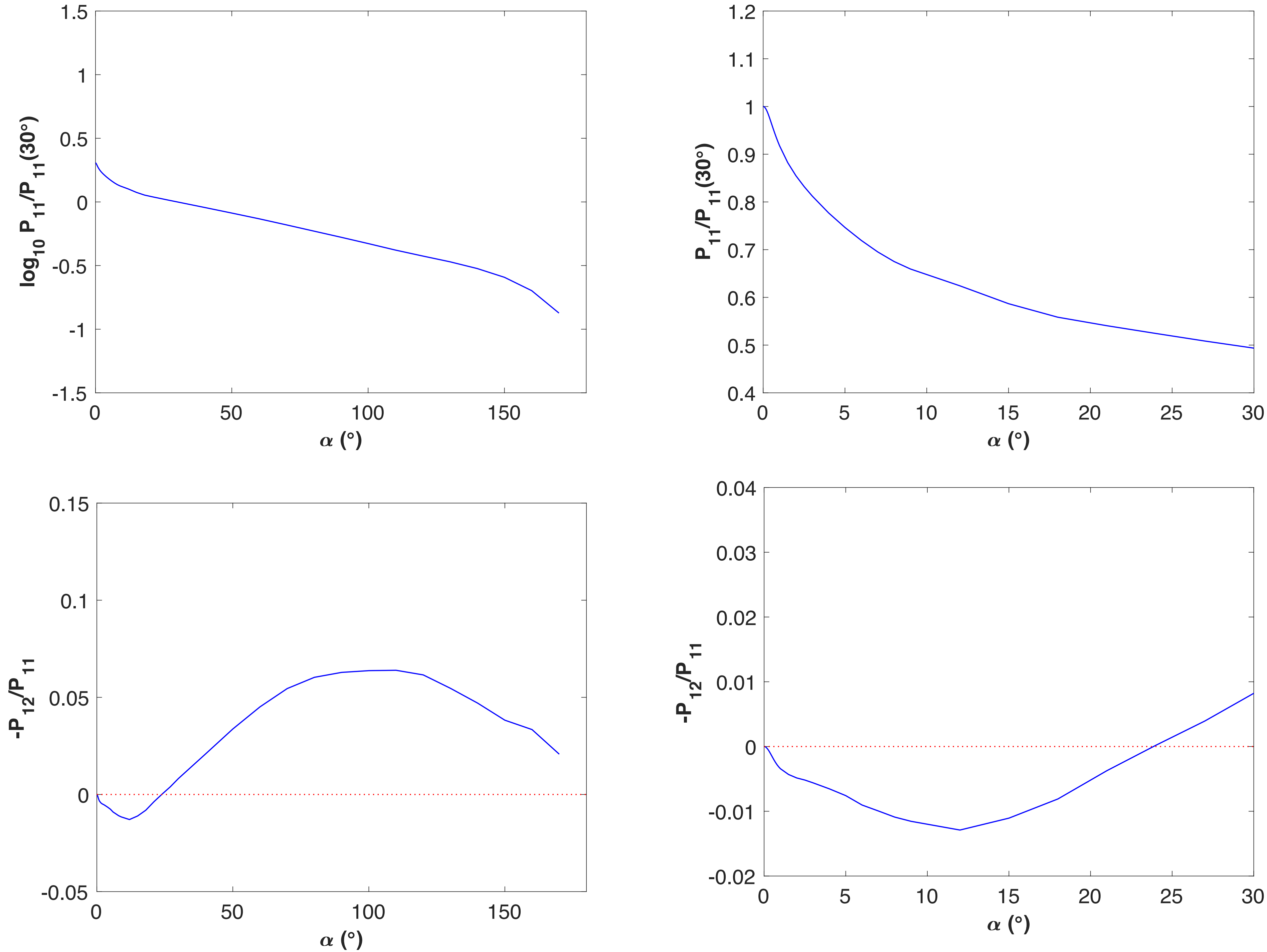

$\log_{10} P_{11}/P_{11}(30°)$
$P_{11}/P_{11}(30°)$
$-P_{12}/P_{11}$
$-P_{12}/P_{11}$
α (°)
α (°)
α (°)
α (°)

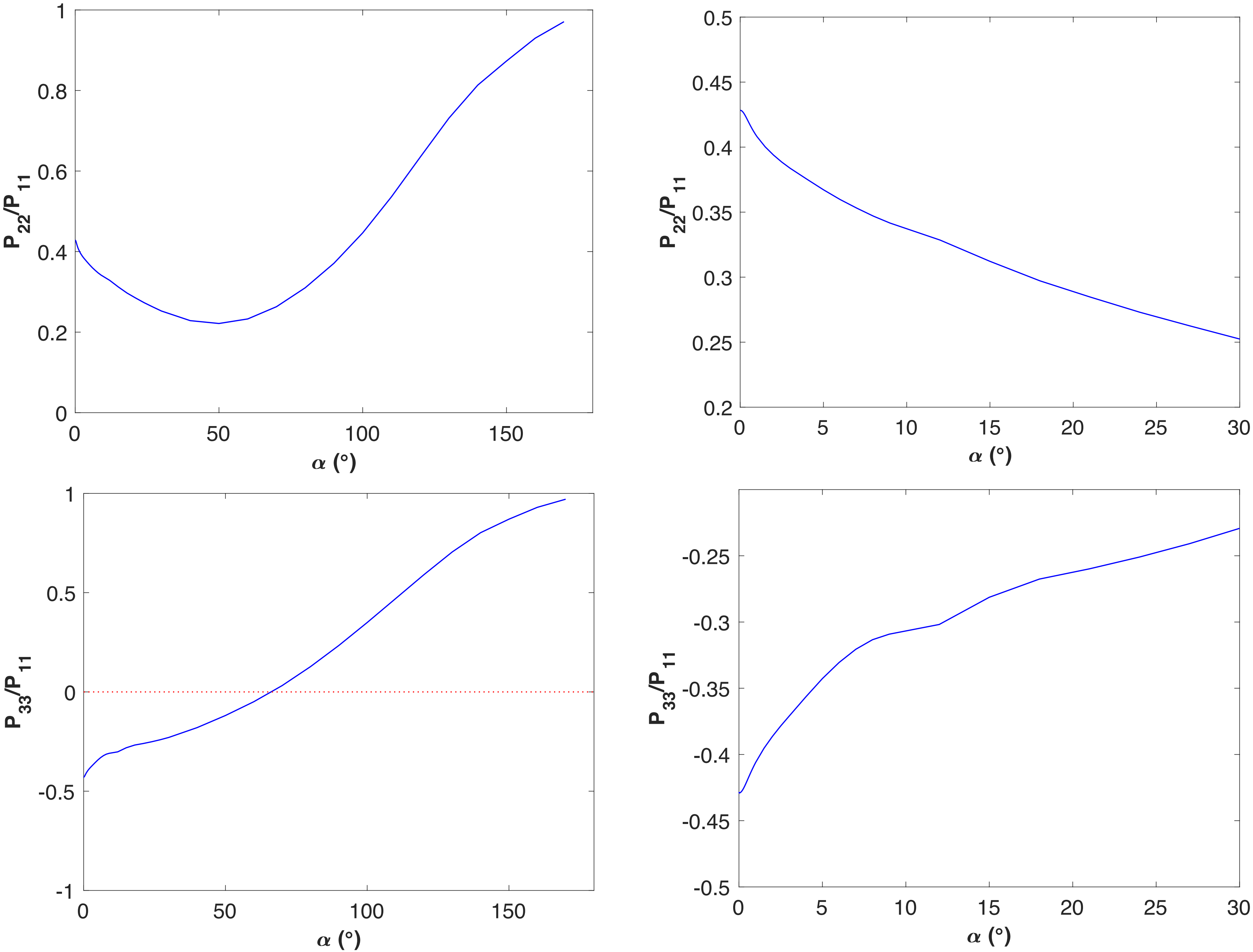

P_{22}/P_{11}
α (°)
P_{22}/P_{11}
α (°)
P_{33}/P_{11}
α (°)
P_{33}/P_{11}
α (°)

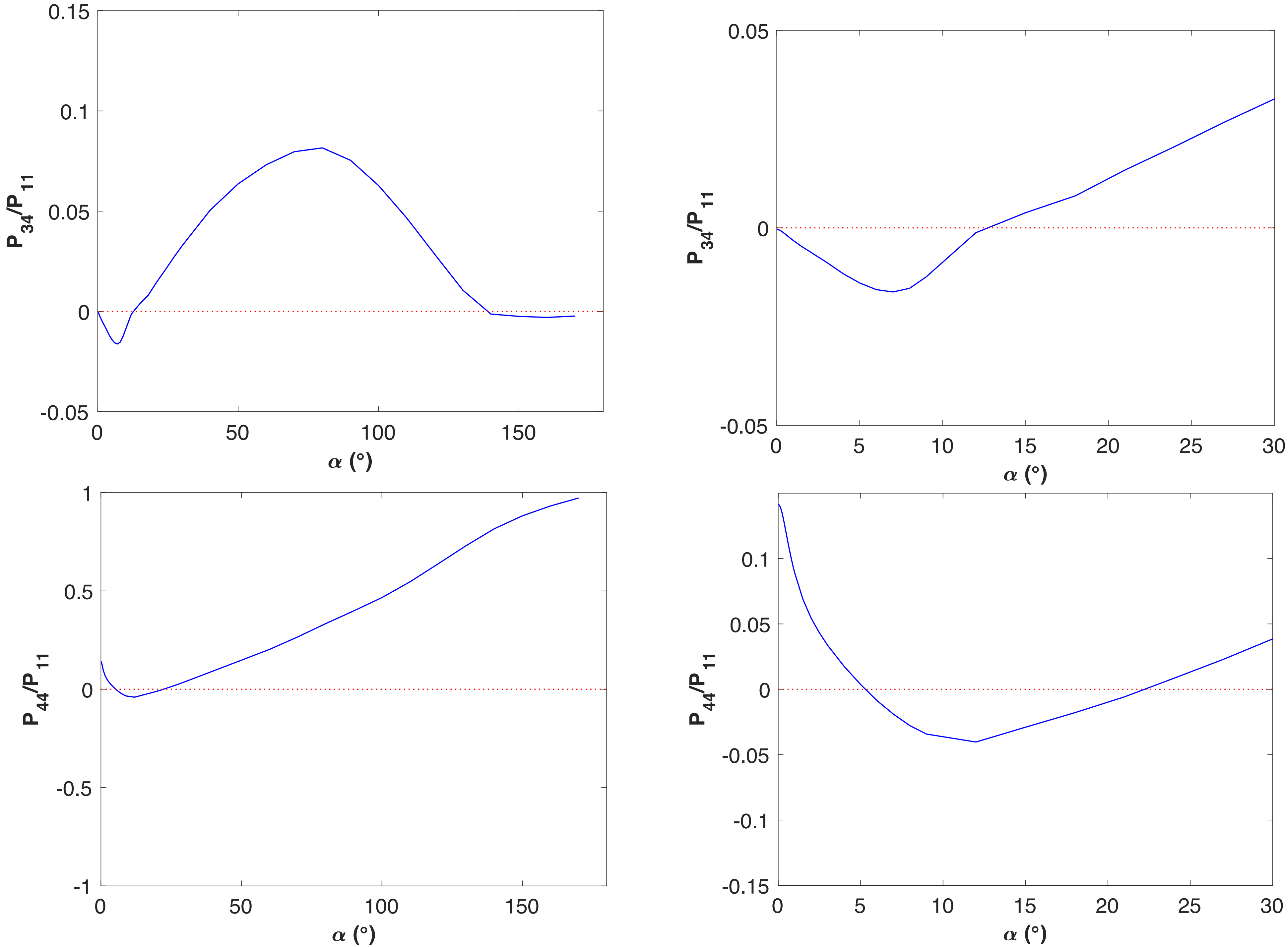

0.15
0.1
0.05
0
-0.05
P34/P11
0
50
100
150
α (°)
0.05
0
-0.05
P34/P11
0
5
10
15
20
25
30
α (°)
1
0.5
0
-0.5
-1
P44/P11
0
50
100
150
α (°)
0.1
0.05
0
-0.05
-0.1
-0.15
P44/P11
0
5
10
15
20
25
30
α (°)

Lunar phase curve: first results

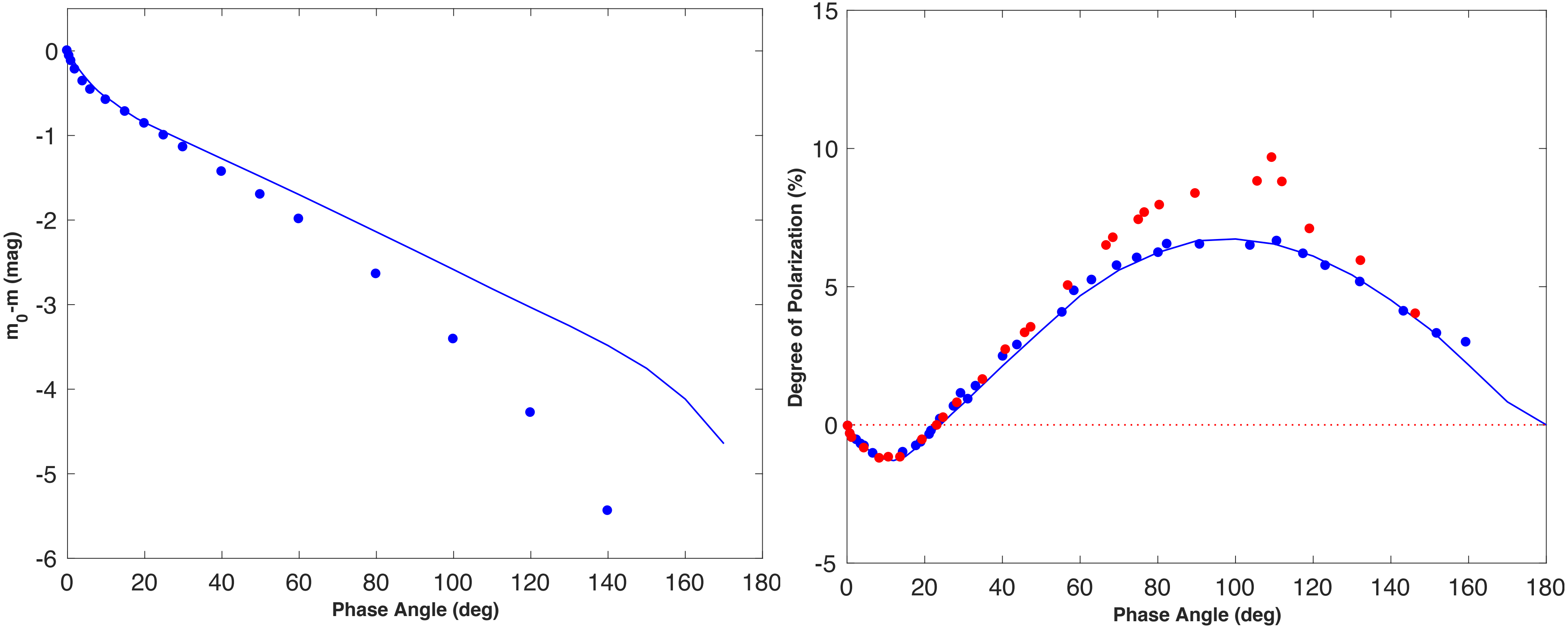

Lunar polarization ratios: first results

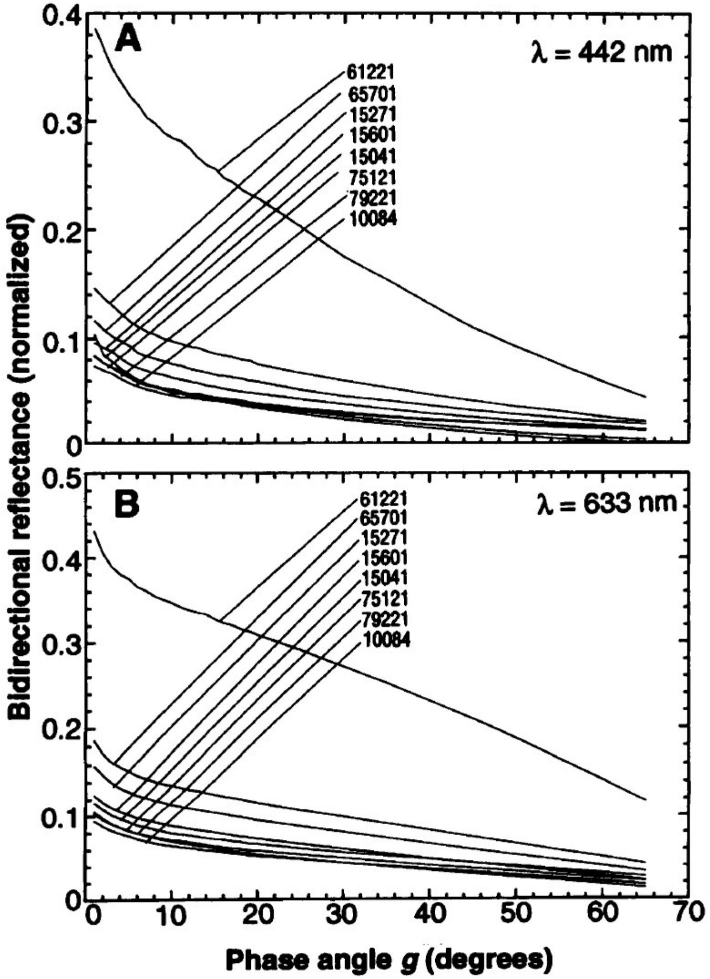

Fig. 1. Bidirectional reflectances of the lunar samples as a function of phase angle *g* in (**A**) blue light and (**B**) red light, normalized to their normal albedos, which are brightnesses relative to a halon standard at an incidence angle of 5°, viewing angle of 10°, and phase angle of 5° (Table 1).

- Laboratory measurements for Apollo samples by Hapke et al. (1993)
- Opposition effect and linear and circular polarization ratios

$$\mu_{\mathrm{L}} = \frac{P_{11} - P_{22}}{P_{11} + 2P_{21} + P_{22}}.$$

$$\mu_{\mathrm{C}} = \frac{P_{11} + P_{44}}{P_{11} - P_{44}}.$$

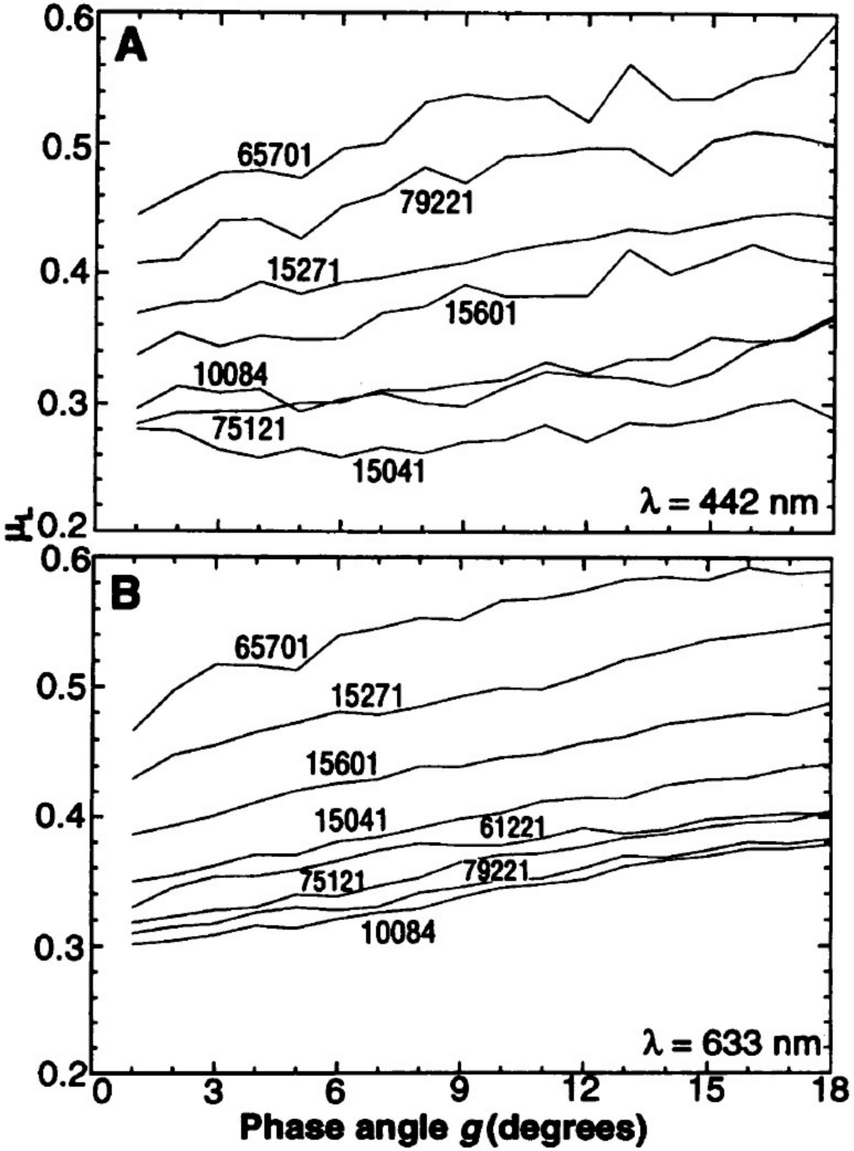

Fig. 2. Linear polarization ratio μ_L versus phase angle g in (**A**) blue light and (**B**) red light. The electric vector of the incident irradiance is perpendicular to the scattering plane (*21*).

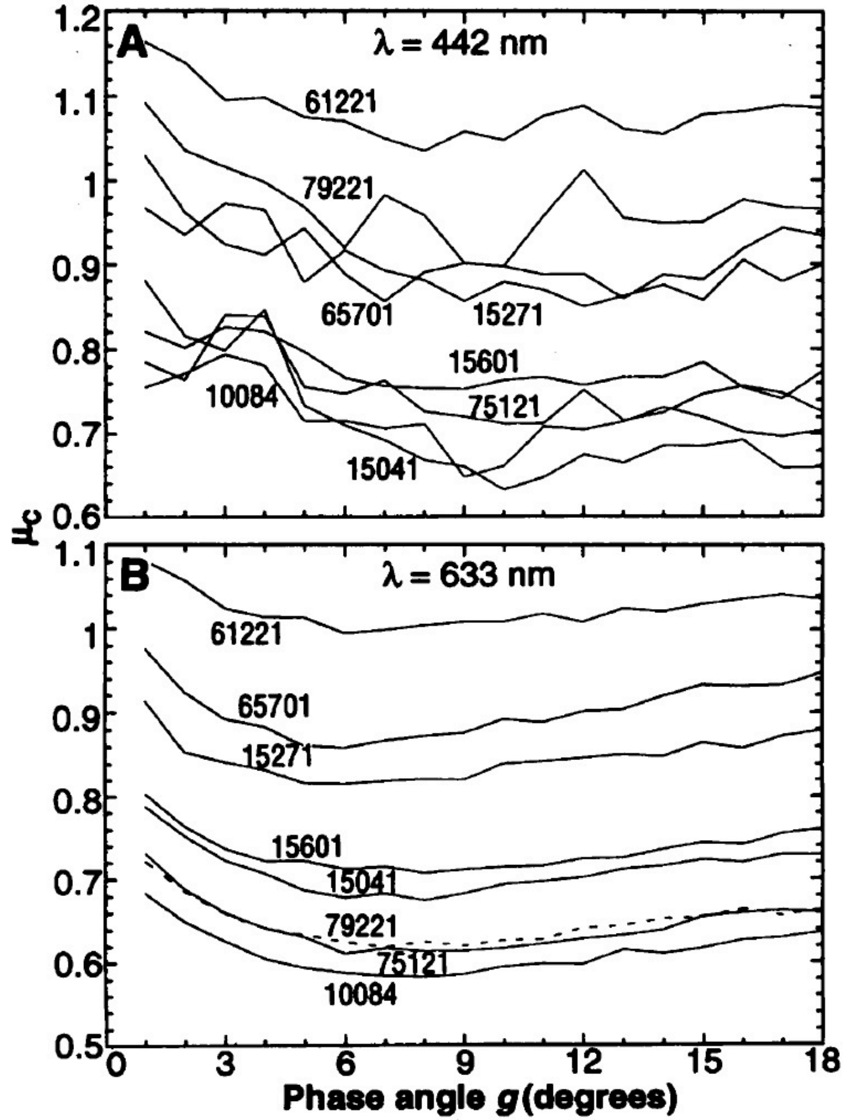

Fig. 3. Circular polarization ratio μ_C versus phase angle g in (**A**) blue light and (**B**) red light. The helicity of the incident irradiance is left-handed (*21*).

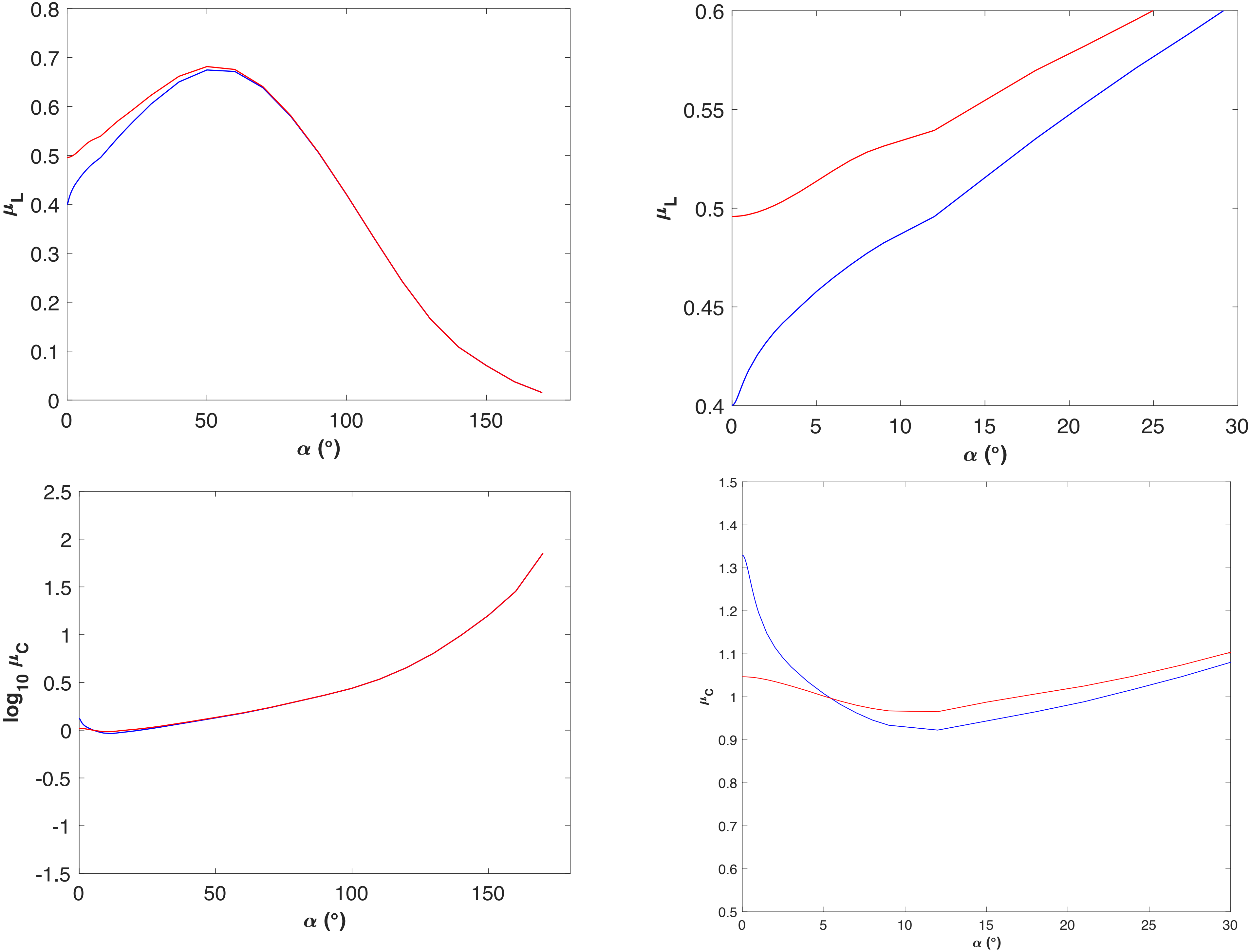

μL
α (°)
log10 μC
μC

Conclusions with future prospects

- Synoptic electromagnetic scattering modeling from first principles
- How do particle size, shape, structure, and composition affect the phase curves and spectra of airless solar system objects?
- What are the prospects for successful inversion?
- Experiments vs. numerical studies vs. observations
- Lunar scattering modeling indicates that
  - interactions among small and large particles key to polarization modeling
  - phase curves introduce constraints on particle size distribution
  - particle shapes constrained by polarization maxima, the value of maximum polarization and and the angle of maximum polarization
  - refractive index constrained by geometric albedo and entire polarization curve
- Prospects for combining modeling and instrumentation